Hydrophobic *versus* Hydrophilic Polyelectrolyte Multilayers for Emissive Europium Films

*Rachel L. Abbett, Rodney A. Tigaa[‡], Swapnil L. Sonawane[§], Geoffrey. F. Strouse, Joseph B. Schlenoff**

Department of Chemistry and Biochemistry, Florida State University, Tallahassee, FL 32306, U.S.A.

Accepted Version *ACS Appl. Polym. Mater.* 2021, 3, 2, 691–698

Present address:

[‡]Department of Physical and Environmental Sciences, Concord University, Athens, WV 24712, U.S.A.

[§]Department of Chemistry, JET's Z. B. Patil College, Dhule 424002, Maharashtra, India

*jschlenoff@fsu.edu

ABSTRACT

Films containing lanthanide ions, having exceptionally narrow emissive bandwidths, are often used for high-performance photonic materials. The lanthanide ion is commonly coordinated with organic ligands to enhance emission intensity. However, the light output is influenced by the environment, such as the presence of water, surrounding the ligated metal center. In this work, hydrophobic and hydrophilic ultrathin polyelectrolyte films made by the multilayering technique were compared as hosts for Eu^{III} tris(dipicolinates), $[Eu(DPA)_3]^{3-}$, complexes. The concentration of complex within the film depended on the number of residual excess positive polyelectrolyte repeat units, which in turn was controlled by the method of multilayer assembly. Because the hydrophobic polyelectrolyte multilayer, PEMU, excluded water more efficiently, the $[Eu(DPA)_3]^{3-}$ emission intensity and lifetime decreased only slightly on exposure of the emissive film to ambient and maintained a quantum yield of 48%.

Keywords: layer-by-layer, self-assembly, display, optical, fluorinated, quantum efficiency.

Introduction

The desire for high-performing photonic materials has resulted in intense research focused on new materials with improved durability and easy manipulation of the site and concentration of emitting dopants.[1] Trivalent lanthanide (Ln^{III}) complexes are preferred for photon emitters due to their sharp line-like emission bands (FWHM = 1 - 10 nm), long emissions lifetimes (μs – ms), and high emission quantum yields.[2] The narrow emission spectra of Ln^{III} ions arise from *f-f* transitions that are forbidden by the Laporte parity rule, which causes the long luminescence lifetimes of the ions.[3, 4] Because *f-f* transitions are forbidden, Ln^{III} ions also have low molar absorptivities (10 M^{-1} cm^{-1}). Thus, Ln^{III} ions such as Eu^{III} are often coordinated with organic ligands that can absorb energy and transfer it to the Ln^{III} ion, leading to metal-centered emission. As a result, there is an increased interest in new ligands with well-matched triplet (^3T) excited-state energy levels to efficiently sensitize Eu^{III}-centered emissions.

Polyelectrolyte multilayers (PEMUs) are ultrathin films made using alternating layer-by-layer deposition of oppositely-charged polyelectrolytes.[5] Interest in these materials has increased in recent years due to the ability to tune their surface charge and for their potential as coatings in industrial applications, including biological implants, optics, sensors, and computer chips.[5, 6, 7, 8, 9, 10, 11, 12, 13] The nature of these systems permits the surface and internal charge content of the system to be finely controlled during and post-production.[14, 15] During growth of a PEMU, an excess of one polyelectrolyte accumulates in the film in a process known as overcompensation, leading to a net charge that can be increased, patterned, or removed.[5, 10, 16, 17, 18, 19, 20, 21, 22, 23, 24, 25, 26, 27] PEMUs provide an opportunity for a structured coating on a surface that could accommodate charged emitters in a controlled manner. The emitters used and their distance from the surface of the substrate are both important considerations for applications requiring a tunable strength of emission. Both factors determine whether the emission is quenched. The emission intensity of these emitters is also affected by their environment and by the presence of any quenchers in the system.[2]

The site environment of an emitting dopant significantly affects the light-matter interactions of the emitter with metallic surfaces. Much research has gone into reducing these interactions, including using polymer systems as scaffolding for emitting dopants.[28, 29, 30, 31, 32, 33, 34, 35, 36] For example, Greenspon et al. demonstrated the incorporation of organometallic Eu^{III} complex into ~17 nm thick PEMUs that showed significant emission intensity even when bound to a plasmonic metal surface.[37] However, the environment and charge density were not controlled to the degree possible, given the current understanding of PEMUs and the variety of polyelectrolytes available. Therefore, there remains a need to develop uniform ultrathin films (< 100 nm) with site-specific deposition of Eu^{III} emitters.

Since PEMUs are made from highly charged components they contain appreciable amounts of water, depending on the humidity of the environment.[12, 38] Because water is an efficient quencher for lanthanides, PEMUs hosting Ln^{III} emitters should be designed for minimal water content.[39, 40, 41, 42, 43, 44] In this work, hydrophobic and hydrophilic PEMUs were prepared and used as frameworks for Eu^{III} tris(dipicolinates), $[Eu(DPA)_3]^{3-}$, complexes to investigate the differences in their effects on the photophysical properties of the Eu^{III} ions. The $[Eu(DPA)_3]^{3-}$ complex was chosen due to its high luminescence quantum yield, high stability and solubility in water, and adaptability to the layer-by-layer assembly method employed in this work. Additionally, the use of $[Eu(DPA)_3]^{3-}$ allows for the environment of the $[Eu(DPA)_3]^{3-}$ complex to be probed optically due to its non-degenerate $^5D_0$ excited state and environment-independent, purely-magnetic $^5D_0 \rightarrow {}^7F_1$ allowed transition.

Materials and Methods

Poly(diallyldimethylammonium chloride) (20% in water, Mw 400,000 - 500,000, PDADMAC), Nafion™ (5% in low aliphatic alcohols and water) , sodium chloride, poly(4-vinyl pyridine) (P4VP, 95%), trifluoroethanol (99%, TFE), 1,1,1,2,2,3,3,4,4-nonafluoro-6-iodohexane (99%), dimethylformamide (99.8%, DMF), 1-bromohexane (98%), diethyl ether (99%) were used as received from Sigma Aldrich. Poly(styrene sulfonic acid) (18% in water, Mw ~75,000, PSS) also from Sigma Aldrich was neutralized to pH 7 with NaOH prior to use. The $Cs_3[Eu(DPA)_3]$ complex was prepared following the procedure described by Brayshaw et al. scaled down by a factor of 3.4.[4]

Synthesis of F-P4VP (Scheme 1): To make P4VP with fluorinated n-alkyl chains, 14.3 mmol of P4VP was dried for 12 h at 110 °C. It was then combined with 5.53 mL 1,1,1,2,2,3,3,4,4-nonafluoro-6-iodohexane and 37 mL dry DMF under Ar and the solution was heated for 24 h at 80 °C (See the first step in Scheme 1). The solution turned dark green within about 2 h). 6 mL 1-bromohexane was added and the reaction was allowed to proceed for a further 24 h under Ar (second step in Scheme 1). The mixture was cooled to room temp then added dropwise into cold diethyl ether at 0 °C to precipitate the alkylated F-P4VP. The compound was filtered, washed with cold ether, and dried at 70 °C for 12 h. FTIR: 1640 and 1472 ($C=N^+$) ring stretching and 1200 – 1300 cm^{-1} C-F stretching vibrations respectively. Elemental analysis, EA, for F-P4VP, first step in Scheme 1, for stoichiometry shown in Scheme 1 %theory (%found): C, 34.96 (33.36); H, 2.6 (2.82); N, 3.45 (3.71); F, 33.75 (28.8); I, 25.07 (30.93). EA for F-P4VP, second step in Scheme 1: C, 35.62 (34.84); H, 3.15 (3.36); N, 3.19 (3.60); F, 31.21 (26.42).

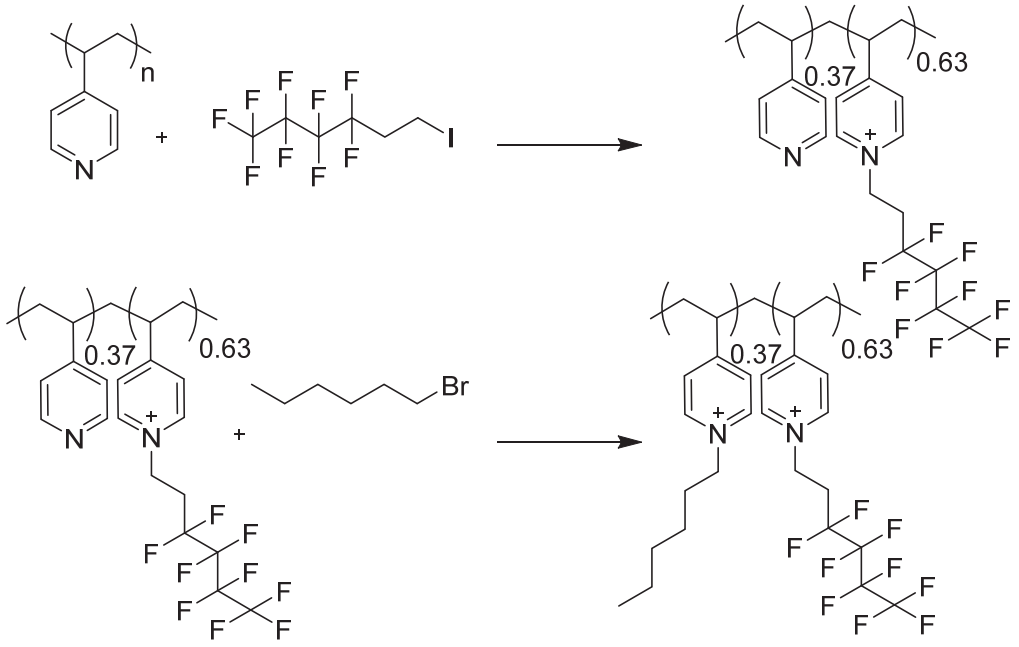

Scheme 1. Reaction scheme for synthesis of F-P4VP. The ratio of fluorinated n-alkyl chains to non-fluorinated chains was determined to be approximately 2:1 by elemental analysis.

Preparation of PEMUs: The polyelectrolyte multilayers were prepared by alternately exposing a substrate to solutions of polycation and polyanion.[45] For the hydrophilic system, 10 mM (concentrations based on the polymer repeat unit) solutions of PDADMA and PSS with 0.5 M NaCl were used. Substrates were dipped for 5 min into polyelectrolyte solutions with three 1-min water rinses between, resulting in 21-layer systems (10.5 “bilayers”), terminated with PDADMA, or 20-layer PEMUs, terminated with PSS. The hydrophobic polymer buildup was

conducted with 10 mM solutions of Nafion and F-P4VP in TFE. Dip times were 5 min with three 1-min TFE rinses between resulting in 20- or 21-layer systems (10.5 bilayer, F-P4VP terminating). PEMUs were built on double side polished Si (100) wafers as well as on quartz slides.

Thickness measurements: Thicknesses were measured using a Gartner Scientific L116 S ellipsometer set at 70 degrees angle of incidence on Si wafers with a refractive index of 3.85, and the sample refractive index set to 1.55 for PDADMA/PSS systems and 1.35 (this refractive index was measured on ~ 100 nm films) for the F-P4VP/Nafion systems. Thicknesses of identically-prepared PEMUs on Si wafers (i.e. terminated with a native SiO_2 layer about 1.5 nm thick) and quartz were assumed to be the same for the same number of bilayers.

FTIR measurements: Transmission FTIR measurements were recorded on a Nicolet Avatar 360 FTIR on double-side-polished Si (100) wafers. Spectra were taken with a dry air purge with 100 scans and a resolution of 4 cm^{-1}. The positive polymer charge content was measured by sorbing nitrate ion (infrared-active) into samples. By immersing the sample in 0.05 M $NaNO_3$ for 1 h, these ions displace the chloride counterions present in the sample. The sample was then quickly rinsed in water and dried under a gentle stream of nitrogen before acquiring another IR spectrum. Vibrational bands used to determine the ion content were from the quarternized ring (1650 cm^{-1}) and nitrate (1450 – 1300 cm^{-1}). The ratio of the nitrate to ring peak area was divided by the ratio from a standard. The standard was N-methylated poly-4-vinyl pyridine (QVP-1). The Br^- counterion in QVP-1 was exchanged with nitrate by precipitating the Br^- with a solution of $AgNO_3$. The IR peak area ratio for the standard was14.10 nitrate/ring.

Excitation and emission measurements: Excitation and emission spectra were recorded at room temp on a Horiba Fluoromax-4 spectrofluorometer equipped with a 450 W Xe lamp and a Peltier-cooled Hamamatsu R928 photomultiplier tube. All spectra were corrected for the instrument response function. Emission lifetime measurements were measured using an Edinburgh FLS980 fluorometer equipped with a 450 W Xe lamp with single grating (1800 λ/mm, 250 nm blaze). The samples were excited with an Nd:YAG laser (Aixiz, AD-532-400T) that was focused through a variable neutral density filter (Edinburgh F-B01 laser mount), a 2 mm diameter iris (Newport ID-1.0) and detected by an intensified Andor iStar CCD camera.

Quantum yield measurements: Quantum yields were measured from samples built on fused silica substrates using the direct excitation method on a Hamamatsu Quantaurus-QY C11347-11 Absolute Photoluminescence Quantum Yield Spectrometer.

Preparation of $[Eu(DPA)_3]^{3-}$ *incorporated in PDADMA/PSS and F-P4VP/Nafion PEMUs:* PDADMA/PSS or F-P4VP/Nafion was deposited on a fused silica slide and immersed in ~1.0 mM aqueous solution of $Cs_3[Eu(DPA)_3]$ for 90 h. The slide was then removed and dried under a gentle stream of nitrogen.

Results and Discussion

Several degrees of control are offered by the narrow-band-emission ultrathin films described here. The thickness of multilayer systems, with a precision of a few nm, is controlled by the number of layers, as shown in the layer-by-layer buildup of the hydrophobic system in Figure S1. Chemical composition determines the hydrophobicity of both the bulk and surface of the multilayer. Though most multilayers are constructed from aqueous solution due to the water-solubility of most polyelectrolytes, layer-by-layer assembly can also be accomplished in organic solvents for sufficiently hydrophobic polyelectrolytes. Fluorinated polymers such as those

employed here, are best assembled in “fluorophilic” solvents, such as TFE.[9] The stoichiometry of polyelectrolyte components within PEMUs is rarely 1:1 positive (Pol^+):negative (Pol^-) repeat units. The multilayer process itself relies on an excess of at least one of the polymers on each layer to reverse the charge and prime the film for the addition of the next layer. In the PDADMA/PSS system, for example, an excess of PDADMA repeat units accumulates within the PEMU.[10]

Charged dopants or ions, including the $[Eu(DPA)_3]^{3-}$ used here, enter the thin film of complexed polyelectrolytes via two routes: at low solution concentration of ion, counterions within the PEMU balancing excess polyelectrolyte may be exchanged. For example, if the PEMU contains 10% excess Pol^+ compensated by chloride ions, these ions may be displaced by dopant ions D^- represented in Equation 1.

$$Pol^+_{1.1}Pol^-_{1.0}Cl^-_{0.1} + 0.1D^- \rightarrow Pol^+_{1.1}Pol^-_{1.0}D^-_{0.1} + 0.1Cl^- \quad [1]$$

At sufficiently high solution ion concentration of salt *CD*, usually above 0.1 M, the PEMU, even if stoichiometric, can be doped with *CD*.

$$Pol^+Pol^- + D^- + C^+ \rightarrow Pol^+D^-Pol^-C^+ \quad [2]$$

In both the hydrophobic and hydrophilic PEMUs employed here, the polycation induces excess positive polymer charge within the PEMU. Thus, PEMUs with an even number of layers (terminated in polyanion) will have fewer Pol^+ sites for DPA anions than those films with an odd number of layers (terminated in polycation).

PEMUs were prepared using the layer-by-layer method as described above using hydrophilic poly(diallyldimethylammonium) and poly(styrene sulfonate) (PDADMA/PSS) and hydrophobic fluorinated poly(4-vinylpyridine) and Nafion (F-P4VP/Nafion) multilayer systems.[46] Although each thickness increment is commonly termed a “layer,” it is known that the polymers are interpenetrating and well mixed or blended on a molecular level.[45] The polymers in the film are thus amorphous, which helps to make them uniform, defect free “hosts” for emissive species.[47] The 3:1 ligand to metal complexes were prepared following literature reports.[4] Luminescent PEMUs were prepared by immersing the thin films (PDADMA/PSS or F-P4VP/Nafion) into 1 mM aqueous solutions of $[Eu(DPA)_3]^{3-}$, which replace resident counterions in the film according to Equation 1. The PEMUs were then quickly dried by gently flowing nitrogen.

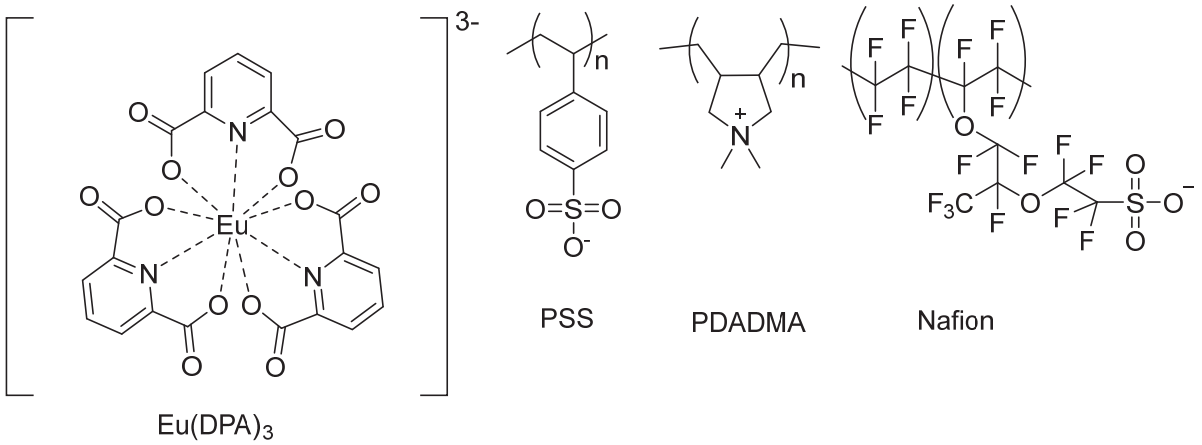

$Eu(DPA)_3$

Figure 1. Structures of $[Eu(DPA)_3]^{3-}$, PDADMA, PSS, and Nafion.

The thicknesses of the 21-layer thin films were measured to be 95 nm for the hydrophilic system, and 47 nm for the hydrophobic system. Prior to their immersion in the $[Eu(DPA)_3]^{3-}$ complex solution, the photophysical properties of the materials were analyzed through a

combination of UV-Vis absorption and fluorescence spectroscopy. The UV-Vis absorption spectra of both the PDADMA/PSS and F-P4VP/Nafion (Figure 1) displayed an absorption band at 270 nm attributed to the aromatic systems in each of the thin films (Figures 1). F-P4VP/Nafion had a significantly higher background (see Figure 2 and Supporting Information Figure S2). Excitation of the thin films at 260 nm resulted in weak blue emission of the materials in the range of 275 - 500 nm. Following uptake of the $[Eu(DPA)_3]^{3-}$ complexes by the PEMUs, additional electronic $\pi \rightarrow \pi^*$ transitions at 280 nm that are attributed to DPA are observed in the absorption spectra (Figure 2).

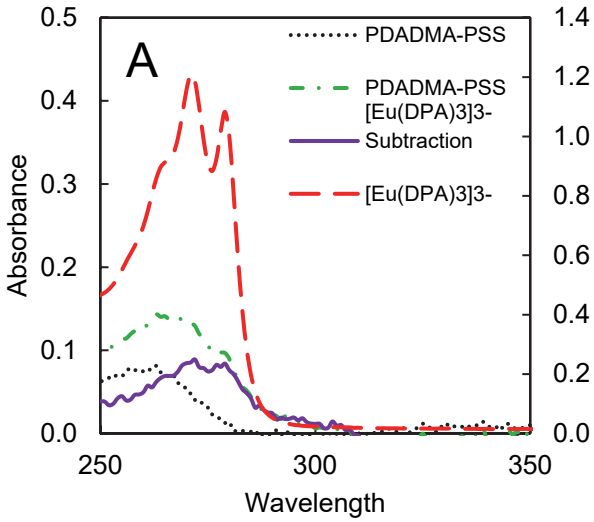

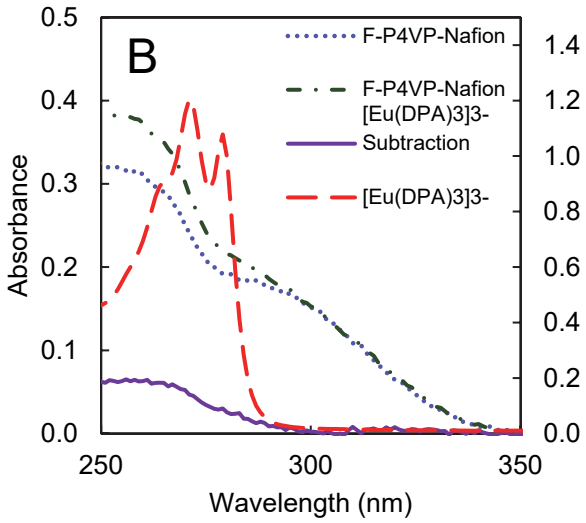

Figure 2. UV-Vis absorption spectra of (A) PDADMA/PSS (95 nm thick) and (B) F-P4VP/Nafion (47 nm thick), along with their respective $[Eu(DPA)_3]^{3-}$-containing systems (absorbance scale is on the left-hand axis). The absorbance for the $[Eu(DPA)_3]^{3-}$ solution spectrum is on the right-hand axis. The difference between respective PEMU and PEMU plus $[Eu(DPA)_3]^{3-}$ spectra are shown as the solid lines. F-P4VP/Nafion exhibits a higher absorbance than PDADMA/PSS over the range shown.

Kinetics of Dopant Uptake

The time-dependent uptake of the $[Eu(DPA)_3]^{3-}$ complexes by the PEMUs was investigated by measuring the emission intensity of the Eu^{III} transitions after extended immersion of the films in 1 mM aqueous solution of $[Eu(DPA)_3]^{3-}$ over time. When excited at 280 nm, typical red Eu^{III} $^5D_0 \rightarrow {}^7F_{J\ (J=0-4)}$ transitions were observed. Monitoring the emission intensity of the Eu^{III} $^5D_0 \rightarrow {}^7F_J$ transitions, it was determined that maximum $[Eu(DPA)_3]^{3-}$uptake occurs rapidly within 5 minutes for the hydrophilic sample, and within 1 hour, plateauing beyond 5 hours for the hydrophobic sample (Figures 3).

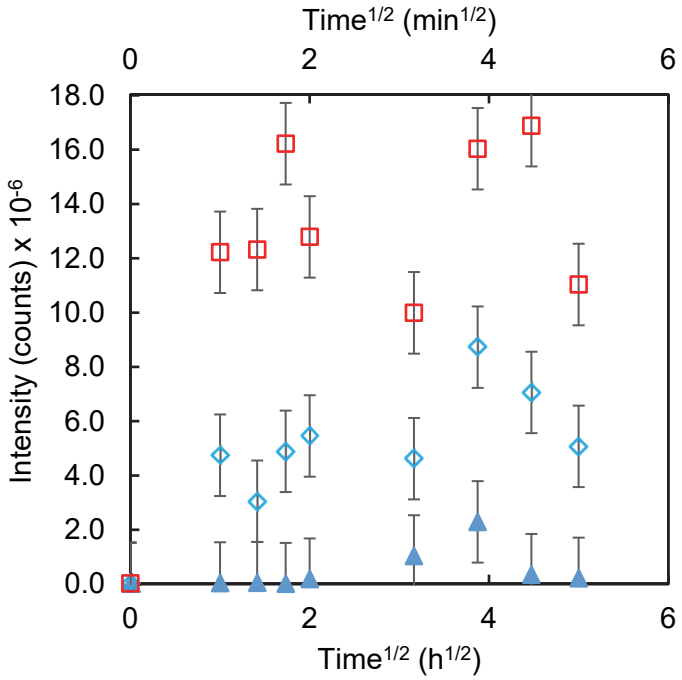

Figure 3. Uptake of $[Eu(DPA)_3]^{3-}$ by 21-layer PDADMA/PSS □ (minutes$^{1/2}$ scale), 21-layer F-P4VP/Nafion ◊ (hours$^{1/2}$ scale), and 20-layer F-P4VP/Nafion ▲ (hours$^{1/2}$) on a quartz slide. The samples were excited at 280 nm while monitoring the emission intensities of the Eu^{III} $^5D_0 \rightarrow {}^7F_2$ transition at 614 nm. Films thicknesses were approximately 95 nm for the hydrophilic system, and 47 nm for the hydrophobic system

When hydrophobic systems were built with 20 layers instead of 21, there was little evidence of uptake of the $[Eu(DPA)_3]^{3-}$ complex in the emission spectra. Though the amount of $[Eu(DPA)_3]^{3-}$ in each film could in principle be estimated from the UV-vis spectra in Figure 2, the high background absorption of F-P4VP/Nafion made reliable subtraction difficult. By labeling the excess charge with $NaNO_3$, the percent excess charge was more reliably determined[48] via transmission FTIR to be 18% for a 21-layer system, compared to previously reported 30% for the hydrophilic system under the same conditions.[10] When the same experiment was conducted for the 20-layer system, no nitrate was seen on the spectra, indicating that the film was not overcompensated by PDADMA (Figure 4). At these ion concentrations, exchange of film ions for solution ions occurs without additional “doping” of the films by solution ions.[48] This demonstrates substantial control of the emitter concentration is possible by the method of PEMU assembly.

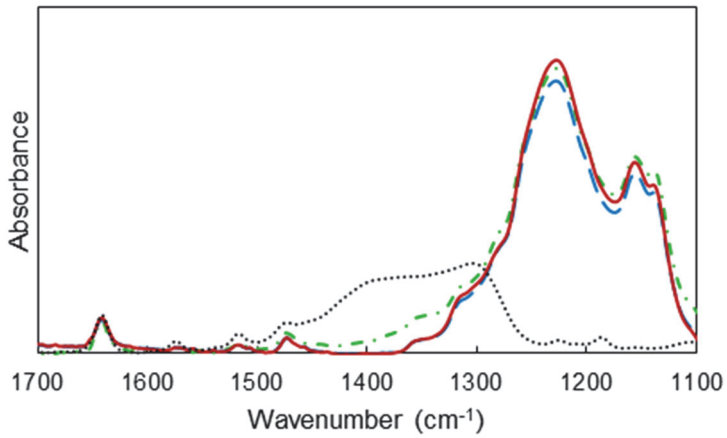

Figure 4. IR spectra of 20- and 21- layer F-P4VP/Nafion film on bare Si wafer, normalized to the 1650 cm^{-1} PVP band, before and after 2 h of exposure to 0.05 M $NaNO_3$ (standard, black dots; 20-layer, red solid line; 20-layer with nitrate, blue dashed line; 21-layer with nitrate, green dash-dot line). Nitrate was used as a label to measure overcompensation. By comparing the nitrate peak area (1450 - 1300 cm^{-1}) to the F-P4VP quaternized ring peak area (1650 cm^{-1}), the degree of overcompensation was determined to be approximately 18% for the 21-layer and 0% for the 20-layer.

Emission of Doped Multilayers

PDADMA/PSS and F-P4VP/Nafion films doped to steady state concentration (Figure 3) with $[Eu(DPA)_3]^{3-}$ were prepared and their photophysical properties studied. The emission maxima of Eu^{III} at 615 nm displayed excitation spectra that overlap the absorption spectrum of the DPA chelator (Figures 2 and 5). The emission transitions observed for the Eu^{III}-containing systems when excited at 280 nm, along with the overlap of the excitation and DPA absorption spectra, indicate that energy was transferred from the DPA ligands to the Eu^{III} ions.

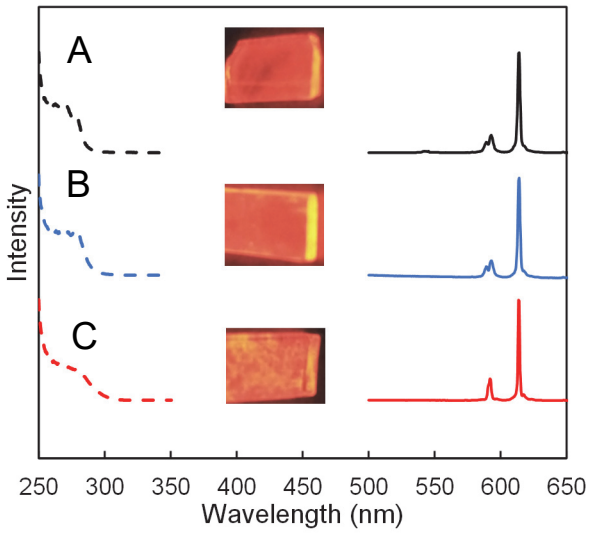

Figure 5. Normalized UV-Vis excitation (left side) and emission (right side) of the $[Eu(DPA)_3]^{3-}$ containing A) F-P4VP/Nafion, B) PDADMA/PSS PEMUs; and C) $Eu(DPA)_3^{3-}$ deposited on fused silica slides. Photographs of each sample under 254 nm UV irradiation on 9 mm wide fused silica are shown in the center.

The quantum yields of the Eu^{III}-containing systems were measured to investigate the effects of the PEMU host environment on the luminescence properties of the $[Eu(DPA)_3]^{3-}$ complexes. The measured absolute emission quantum yields for the Eu^{III}-containing systems were 22% for the PDADMA/PSS films and 48% for the F-P4VP/Nafion films respectively, when excited at 280 nm (Table 1). The quantum yield of the hydrophilic PDADMA/PSS system is comparable to the value of $[Eu(DPA)_3]^{3-}$ (24%) complexes in Tris/HCl buffer (pH = 7.4).[3] The emission efficiency of $Eu(DPA)_3^{3-}$ complex drop-cast onto a quartz slide was significantly higher than the solution samples, reaching an absolute emission efficiency of 63% (Table 1). This value is similar to reports by Mooibroek and co-workers who measured emission efficiencies of 72% for the Eu^{III} solid samples following excitation at 254 nm.[49]

Table 1. The emission lifetime, τ_{obs}, and overall Φ_{Ln}^{L}, quantum yields of the $[Eu(DPA)_3]^{3-}$ complex dried and in water, along with the PDADMA/PSS and F-P4VP/Nafion PEMUs doped with $Eu(DPA)_3^{3-}$ on fused silica slides. $[Eu(DPA)_3]^{3-}$ excitation wavelength was 280 nm while the monitored emission wavelength was 614 nm.

Sample	τ_{obs} [ms]	Φ_{Ln}^{L} [%]
Drop cast $[Eu(DPA)_3]^{3-}$	1.73±0.03	63.1±3.0
$[Eu(DPA)_3]^{3-}$ in Tris/HCl Buffer	1.67±0.03	24.0±2.5
PDADMA/PSS + $[Eu(DPA)_3]^{3-}$	1.84±0.01	22.3±4.8
F-P4VP/Nafion + $[Eu(DPA)_3]^{3-}$	1.85±0.01	48.4±3.3
0% humidity PDADMA/PSS + $[Eu(DPA)_3]^{3-}$	2.38±0.01	--
0% humidity F-P4VP/Nafion + $[Eu(DPA)_3]^{3-}$	1.91±0.01	--

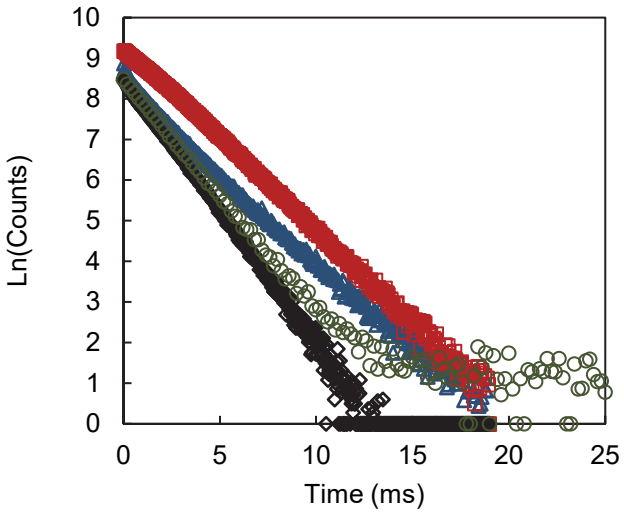

Figure 6. Emission decay curves of the $[Eu(DPA)_3]^{3-}$ complex and $[Eu(DPA)_3]^{3-}$ containing PEMUs. Every 5 data points were averaged.

Analysis of the photophysical data provided further insight into the effect of the PEMU environment on the Eu^{III} emission efficiency. The emission quantum yield of the $[Eu(DPA)_3]^{3-}$ complex decreased by approximately 40% and 15% compared to dry $[Eu(DPA)_3]^{3-}$ alone when incorporated into the hydrophilic PDADMA/PSS and the hydrophobic F-P4VP/Nafion films (Table 1). This can be attributed to the stronger non-radiative quenching from the O-H oscillators (water) in the hydrophilic film compared to the hydrophobic film. Emission lifetime measurements were conducted by exciting at 280 nm and monitoring the $^5D_0 \rightarrow {}^7F_2$ (615 nm) transitions of Eu^{III}. The emission decay curves of the $[Eu(DPA)_3]^{3-}$ fit mono-exponential functions, which indicate that the Eu^{III} ions occupy a single environment (Figure 6). The measured emission lifetime, τ_{615}, of the drop cast $[Eu(DPA)_3]^{3-}$ complex (1.73 ms) are comparable to literature values $[Eu(DPA)_3]^{3-}$ = 2.06 ms).[49] Following incorporation of the $[Eu(DPA)_3]^{3-}$ complexes into the films, the τ_{615} was 1.84 ms for the PDADMA/PSS samples, while τ_{615} of doped F-P4VP/Nafion was 1.85 ms (Table 1). The higher emission lifetime following incorporation of the $[Eu(DPA)_3]^{3-}$ complexes into the films can be attributed to improved water shielding by the films. The decay curves of the multilayers containing $[Eu(DPA)_3]^{3-}$ also fit mono-exponential functions which indicates that the Eu^{III} ions occupy a similar environment, even after embedding in the films (Figure 6). Incorporation of the $[Eu(DPA)_3]^{3-}$ complexes into the films did not show any significant effect on the color purity of the Eu^{III} emission as the linewidths (FWHM) of the $^5D_0 \rightarrow {}^7F_2$ were determined to be minimally broadened from 2.2(± 0.1) nm to 2.4 nm when incorporated into the F-P4VP/Nafion and PDADMA/PSS films. The ratio, R/O, of the intensities of the red $^5D_0 \rightarrow {}^7F_2$ and orange $^5D_0 \rightarrow {}^7F_1$ transitions of Eu^{III} can be used to gain insight into the local symmetry of the Eu^{III} ions in the films.[50] This is because the $^5D_0 \rightarrow {}^7F_2$ is a hypersensitive transition and can be altered by the Eu^{III} environment. The analysis of $Eu(DPA)_3$-containing films revealed that the Eu^{III} ions remained coordinated to the DPA ligands as the R/O values for the metal complexes (3.8), PDADMA/PSS (3.6) and F-P4VP/Nafion (3.7) luminescent films were similar.[51, 52]

Influence of Hydration on Photophysical Properties

Photophysical studies were also conducted to evaluate the change of emission intensity in both the hydrophobic and hydrophilic PEMUs on exposure to an environment that contains water. $[Eu(DPA)_3]^{3-}$ PEMU samples were dried at 120 °C and transferred to a glovebox to remove bound and unbound water from the system. The samples were sealed in fused silica cuvettes

with threaded caps that were sealed with parafilm. On exposure to ambient conditions (about 25 °C and 45% relative humidity) water uptake in the hydrophilic systems was almost instantaneous with a drop in the emission intensity (Figure 7) and emission lifetime (Figure 8)over 10 min of data collection. However, no changes in the emission intensity or lifetime of the hydrophobic PEMU system were observed on exposure to the same ambient conditions (Figures 7 and 8). After the water content at ambient stabilized, the samples were submerged briefly in water. Excess water on the surface of the samples was removed, and intensity measurements were taken. The hydrophobic system exhibited a more drastic drop in intensity than the hydrophilic system (Figure 7). After drying the samples again the hydrophilic sample recovered full emission intensity and the hydrophobic sample recovered about 70%.

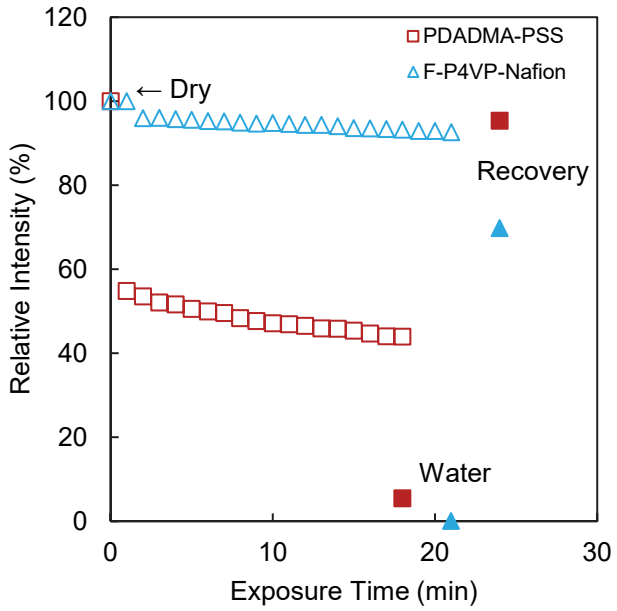

Figure 7. Plot of relative Eu^{III} emission intensity as a function of air exposure time of the $[Eu(DPA)_3]^{3-}$containing films of PDADMA/PSS and F-P4VP/Nafion deposited on a fused silica slide at 614 nm. Initial intensities were 1.15 x 10^7 and 7.42 x 10^7 counts for PDADMA/PSS and F-P4VP/Nafion respectively. 45% relative humidity and 25 °C. The first set of solid points correspond to relative intensity after immersion in water. The last set of solid points correspond to recovery of emission after the films were dried again.

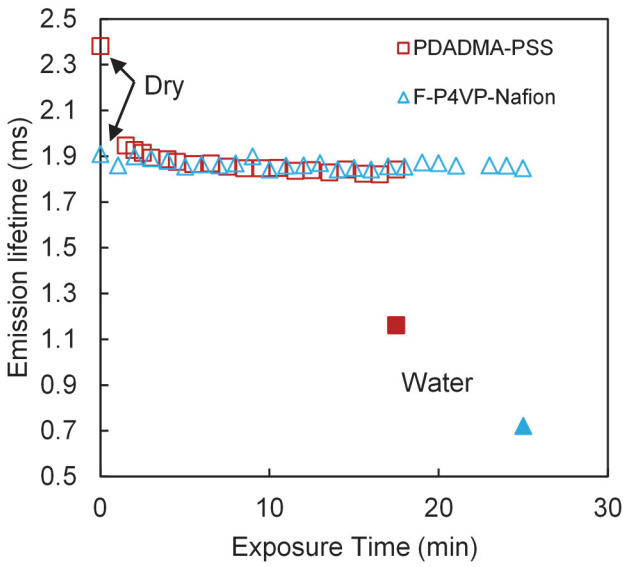

Figure 8. Eu^{III} emission lifetimes as a function of air exposure time of the $[Eu(DPA)_3]^{3-}$-containing PEMUs. The samples were excited at 280 nm while the emission was monitored at 614 nm. Experiment was conducted at 45% relative humidity and 25 °C. The last points (solid) correspond to lifetime following immersion in water.

Conclusions

Eu^{III} complexes were embedded into polyelectrolyte multilayers to generate highly luminescent films. The concentration of these $[Eu(DPA)_3]^{3-}$ emissive centers was determined by the concentration of excess positive polyelectrolyte. Thus, films terminated with polyanion captured much less complex. The hydrophobic film provided a good environment for these complexes, with a measured absolute quantum yield of 48%, compared to 22% measured for the hydrophilic film. Hydrophilic films were faster to take up Eu^{III} complex, requiring only 5 minutes to reach saturation. In contrast, uptake of the Eu^{III} complex by the hydrophobic film was slow, requiring up to 5 hours. However, the emission properties of Eu^{III} complex hosted by hydrophobic film, were compromised far less by exposure to humid atmosphere, showing just 7% decrease in emission lifetime. This work offers a new avenue for designing and fabricating environmentally stable high performing luminescent films for applications in imaging and sensing.

Supporting Information

Layer by layer buildup of hydrophobic film; solution absorption spectrum of PSS and F-P4VP; FTIR spectra of PDADMA/PSS and F-P4VP/Nafion PEMUs in ambient humidity (55% at 19 ºC) showing much lower water content of the latter; FTIR spectra of alkylated P4VP; expanded images of $[Eu(DPA)_3]^{3-}$incorporated in PDADMA/PSS, drop-cast $Eu(DPA)_3$, and F-P4VP/Nafion under irradiation at 254 nm; IR spectra of 20- and 21- layer PDADMA/PSS film on Si wafer before and after exposure to 0.05 M $NaNO_3$ illustrating greater uptake of nitrate for the latter. This information is available free of charge.

Acknowledgement

This work was supported by grant DMR-1809304 from the National Science Foundation.

ORCID IDs

Rachel L. Abbett: 0000-0002-4019-4925

Rodney A. Tigaa − 0000-0001-8976-168X

Swapnil L. Sonawane: 0000-0002-6123-9053

Geoffrey F. Strouse: 0000-0003-0841-282X

Joseph B. Schlenoff: 0000-0001-5588-1253

References

1. Bünzli, J.-C. G. Lanthanide Luminescence for Biomedical Analyses and Imaging. *Chem. Rev.* **2010,** *110*, 2729-2755.
2. Zhang, K. Y.; Yu, Q.; Wei, H.; Liu, S.; Zhao, Q.; Huang, W. Long-Lived Emissive Probes for Time-Resolved Photoluminescence Bioimaging and Biosensing. *Chemical Reviews* **2018,** *118*, 1770-1839.
3. Bünzli, J.-C. G.; Eliseeva, S. V. Intriguing Aspects of Lanthanide Luminescence. *Chemical Science* **2013,** *4*, 1939-1949.
4. Brayshaw, P. A.; Bünzli, J.-C. G.; Froidevaux, P.; Harrowfield, J. M.; Kim, Y.; Sobolev, A. N. Synthetic, Structural, and Spectroscopic Studies on Solids Containing Tris(Dipicolinato) Rare Earth Anions and Transition or Main Group Metal Cations. *Inorganic Chemistry* **1995,** *34*, 2068-2076.
5. Dubas, S. T.; Schlenoff, J. B. Factors Controlling the Growth of Polyelectrolyte Multilayers. *Macromolecules* **1999,** *32*, 8153-8160.
6. Salomäki, M.; Tervasmäki, P.; Areva, S.; Kankare, J. The Hofmeister Anion Effect and the Growth of Polyelectrolyte Multilayers. *Langmuir* **2004,** *20*, 3679-3683.
7. Jisr, R. M.; Rmaile, H. H.; Schlenoff, J. B. Hydrophobic and Ultrahydrophobic Multilayer Thin Films from Perfluorinated Polyelectrolytes. *Angewandte Chemie International Edition* **2005,** *44*, 782-785.
8. Boudou, T.; Crouzier, T.; Ren, K.; Blin, G.; Picart, C. Multiple Functionalities of Polyelectrolyte Multilayer Films: New Biomedical Applications. *Advanced Materials* **2010,** *22*, 441-467.
9. Guillaume-Gentil, O.; Akiyama, Y.; Schuler, M.; Tang, C.; Textor, M.; Yamato, M.; Okano, T.; Vörös, J. Polyelectrolyte Coatings with a Potential for Electronic Control and Cell Sheet Engineering. *Advanced Materials* **2008,** *20*, 560-565.
10. Ghostine, R. A.; Markarian, M. Z.; Schlenoff, J. B. Asymmetric Growth in Polyelectrolyte Multilayers. *Journal of the American Chemical Society* **2013,** *135*, 7636-7646.
11. Milkova, V.; Kamburova, K.; Radeva, T. Electro-Optics of Polyelectrolyte Multilayers on Colloidal Particles. *Colloids and Surfaces A: Physicochemical and Engineering Aspects* **2014,** *460*, 502-509.
12. Nikolaev, K. G.; Ulasevich, S. A.; Luneva, O.; Orlova, O. Y.; Vasileva, D.; Vasilev, S.; Novikov, A. S.; Skorb, E. V. Humidity-Driven Transparent Holographic Free-Standing Polyelectrolyte Films. *ACS Applied Polymer Materials* **2020,** *2*, 105-112.
13. Li, X.; Zhang, X.; Wang, N.; Chang, H.; Wang, Y.; Zhang, Z. Range-Broadening Ultraviolet-Blocking Regulation of Cellulose Nanopaper Via Surface Self-Absorption with Poly(Methyl Methacrylate)/Avobenzone. *ACS Applied Polymer Materials* **2019,** *1*, 2981-2989.
14. Delgado, J. D.; Surmaitis, R. L.; Abou Shaheen, S.; Schlenoff, J. B. Engineering Thiolated Surfaces with Polyelectrolyte Multilayers. *ACS Applied Materials & Interfaces* **2019,** *11*, 3524-3535.
15. Kelly, K. D.; Fares, H. M.; Abou Shaheen, S.; Schlenoff, J. B. Intrinsic Properties of Polyelectrolyte Multilayer Membranes: Erasing the Memory of the Interface. *Langmuir* **2018,** *34*, 3874-3883.

16. Dubas, S. T.; Schlenoff, J. B. Swelling and Smoothing of Polyelectrolyte Multilayers by Salt. *Langmuir* **2001,** *17*, 7725-7727.
17. Guzmán, E.; Ritacco, H.; Rubio, J. E. F.; Rubio, R. G.; Ortega, F. Salt-Induced Changes in the Growth of Polyelectrolyte Layers of Poly(Diallyl-Dimethylammonium Chloride) and Poly(4-Styrene Sulfonate of Sodium). *Soft Matter* **2009,** *5*, 2130.
18. Han, L.; Mao, Z.; Wuliyasu, H.; Wu, J.; Gong, X.; Yang, Y.; Gao, C. Modulating the Structure and Properties of Poly(Sodium 4-Styrenesulfonate)/Poly(Diallyldimethylammonium Chloride) Multilayers with Concentrated Salt Solutions. *Langmuir* **2012,** *28*, 193-199.
19. Hoogeveen, N. G.; Cohen Stuart, M. A.; Fleer, G. J.; Böhmer, M. R. Formation and Stability of Multilayers of Polyelectrolytes. *Langmuir* **1996,** *12*, 3675-3681.
20. Hübsch, E.; Ball, V.; Senger, B.; Decher, G.; Voegel, J.-C.; Schaaf, P. Controlling the Growth Regime of Polyelectrolyte Multilayer Films: Changing from Exponential to Linear Growth by Adjusting the Composition of Polyelectrolyte Mixtures. *Langmuir* **2004,** *20*, 1980-1985.
21. Kovacevic, D.; van der Burgh, S.; de Keizer, A.; Cohen Stuart, M. A. Kinetics of Formation and Dissolution of Weak Polyelectrolyte Multilayers: Role of Salt and Free Polyions. *Langmuir* **2002,** *18*, 5607-5612.
22. Lösche, M.; Schmitt, J.; Decher, G.; Bouwman, W. G.; Kjaer, K. Detailed Structure of Molecularly Thin Polyelectrolyte Multilayer Films on Solid Substrates as Revealed by Neutron Reflectometry. *Macromolecules* **1998,** *31*, 8893-8906.
23. Owusu-Nkwantabisah, S.; Gammana, M.; Tripp, C. P. Dynamics of Layer-by-Layer Growth of a Polyelectrolyte Multilayer Studied in Situ Using Attenuated Total Reflectance Infrared Spectroscopy. *Langmuir* **2014,** *30*, 11696-11703.
24. Picart, C.; Mutterer, J.; Richert, L.; Luo, Y.; Prestwich, G. D.; Schaaf, P.; Voegel, J. C.; Lavalle, P. Molecular Basis for the Explanation of the Exponential Growth of Polyelectrolyte Multilayers. *Proceedings of the National Academy of Sciences* **2002,** *99*, 12531-12535.
25. Porcel, C.; Lavalle, P.; Ball, V.; Decher, G.; Senger, B.; Voegel, J.-C.; Schaaf, P. From Exponential to Linear Growth in Polyelectrolyte Multilayers. *Langmuir* **2006,** *22*, 4376-4383.
26. Schmitt, J.; Gruenewald, T.; Decher, G.; Pershan, P. S.; Kjaer, K.; Löesche, M. Internal Structure of Layer-by-Layer Adsorbed Polyelectrolyte Films: A Neutron and X-Ray Reflectivity Study. *Macromolecules* **1993,** *26*, 7058-7063.
27. Schlenoff, J. B.; Ly, H.; Li, M. Charge and Mass Balance in Polyelectrolyte Multilayers. *Journal of the American Chemical Society* **1998,** *120*, 7626-7634.
28. Yamamoto, M.; Ando, K.; Inoue, M.; Kanoh, H.; Yamagami, M.; Wakiya, T.; Iida, E.; Taniguchi, T.; Kishikawa, K.; Kohri, M. Poly-B-Ketoester Particles as a Versatile Scaffold for Lanthanide-Doped Colorless Magnetic Materials. *ACS Applied Polymer Materials* **2020**, *2*, 2170-2178.
29. Song, X.-Q.; Meng, H.-H.; Lin, Z.-G.; Wang, L. 2D Lanthanide Coordination Polymers: Synthesis, Structure, Luminescent Properties, and Ratiometric Sensing Application in the Hydrostable Pmma-Doped Hybrid Films. *ACS Applied Polymer Materials* **2020,** *2*, 1644-1655.
30. Vikrant, K.; Tsang, D. C. W.; Raza, N.; Giri, B. S.; Kukkar, D.; Kim, K.-H. Potential Utility of Metal–Organic Framework-Based Platform for Sensing Pesticides. *ACS Applied Materials & Interfaces* **2018,** *10*, 8797-8817.
31. Kohri, M.; Yanagimoto, K.; Kohaku, K.; Shiomoto, S.; Kobayashi, M.; Imai, A.; Shiba, F.; Taniguchi, T.; Kishikawa, K. Magnetically Responsive Polymer Network Constructed by Poly(Acrylic Acid) and Holmium. *Macromolecules* **2018,** *51*, 6740-6745.
32. Abdallah, A.; Daiguebonne, C.; Suffren, Y.; Rojo, A.; Demange, V.; Bernot, K.; Calvez, G.; Guillou, O. Microcrystalline Core–Shell Lanthanide-Based Coordination Polymers for Unprecedented Luminescent Properties. *Inorganic Chemistry* **2019,** *58*, 1317-1329.

33. Khomutov, G. B.; Beresneva, I. V.; Bykov, I. V.; Gainutdinov, R. V.; Koksharov, Y. A.; Mantsyzov, B. I.; Masselin, P.; Ozheredov, I. A.; Radchenko, I. L.; Shkurinov, A. P.; Tolstikhina, A. L. Formation of Polymer Films Containing Multivalent Metal Cations by Stepwise Alternate Adsorption of Metal Cations and Polyanions. *Colloids and Surfaces A: Physicochemical and Engineering Aspects* **2002,** *198-200*, 491-499.
34. S. L. V. Narayana, Y.; Yoshida, T.; Chakraborty, C.; Bera, M. K.; Higuchi, M. Proton Conductivity of Metallo-Supramolecular Polymer Boosted by Lithium Ions. *ACS Applied Polymer Materials* **2020,** *2*, 326-334.
35. Kohaku, K.; Inoue, M.; Kanoh, H.; Taniguchi, T.; Kishikawa, K.; Kohri, M. Full-Color Magnetic Nanoparticles Based on Holmium-Doped Polymers. *ACS Applied Polymer Materials* **2020**, *2*, 1800-1806.
36. Hamdalla, T. A.; Hanafy, T. A.; Seleim, S. M. Effect of Rare Earth Elements on the Structural and Optical Properties of Pmma for Possible Uses in Polymer Optical Communications. *Phase Transitions* **2019,** *92*, 603-613.
37. Greenspon, A. S.; Marceaux, B. L.; Hu, E. L. Robust Lanthanide Emitters in Polyelectrolyte Thin Films for Photonic Applications. *Nanotechnology* **2018,** *29*, 075302.
38. Lyu, X.; Peterson, A. M. Humidity Tempering of Polyelectrolyte Complexes. *Macromolecules* **2018,** *51*, 10003-10010.
39. Batys, P.; Zhang, Y.; Lutkenhaus, J. L.; Sammalkorpi, M. Hydration and Temperature Response of Water Mobility in Poly(Diallyldimethylammonium)–Poly(Sodium 4-Styrenesulfonate) Complexes. *Macromolecules* **2018,** *51*, 8268-8277.
40. Fares, H. M.; Wang, Q.; Yang, M.; Schlenoff, J. B. Swelling and Inflation in Polyelectrolyte Complexes. *Macromolecules* **2019,** *52*, 610-619.
41. Eneh, C. I.; Bolen, M. J.; Suarez-Martinez, P. C.; Bachmann, A. L.; Zimudzi, T. J.; Hickner, M. A.; Batys, P.; Sammalkorpi, M.; Lutkenhaus, J. L. Fourier Transform Infrared Spectroscopy Investigation of Water Microenvironments in Polyelectrolyte Multilayers at Varying Temperatures. *Soft Matter* **2020,** *16*, 2291-2300.
42. Zhang, Y.; Batys, P.; O'Neal, J. T.; Li, F.; Sammalkorpi, M.; Lutkenhaus, J. L. Molecular Origin of the Glass Transition in Polyelectrolyte Assemblies. *ACS Central Science* **2018,** *4*, 638-644.
43. Schlenoff, J. B. Site-Specific Perspective on Interactions in Polyelectrolyte Complexes: Toward Quantitative Understanding. *The Journal of Chemical Physics* **2018,** *149*, 163314.
44. Ostendorf, A.; Schönhoff, M.; Cramer, C. Ionic Conductivity of Solid Polyelectrolyte Complexes with Varying Water Content: Application of the Dynamic Structure Model. *Physical Chemistry Chemical Physics* **2019,** *21*, 7321-7329.
45. Decher, G. Fuzzy Nanoassemblies: Toward Layered Polymeric Multicomposites. *Science* **1997,** *277*, 1232-1237.
46. Fares, H. M.; Schlenoff, J. B. Diffusion of Sites Versus Polymers in Polyelectrolyte Complexes and Multilayers. *Journal of the American Chemical Society* **2017,** *139*, 14656-14667.
47. Ball, V. Organic and Inorganic Dyes in Polyelectrolyte Multilayer Films. *Materials* **2012,** *5*, 2681-2704.
48. Schlenoff, J. B.; Rmaile, A. H.; Bucur, C. B. Hydration Contributions to Association in Polyelectrolyte Multilayers and Complexes: Visualizing Hydrophobicity. *Journal of the American Chemical Society* **2008,** *130*, 13589-13597.
49. Mooibroek, T. J.; Gamez, P.; Pevec, A.; Kasunič, M.; Kozlevčar, B.; Fu, W.-T.; Reedijk, J. Efficient, Stable, Tunable, and Easy to Synthesize, Handle and Recycle Luminescent Materials: $[H_2nme_2]_3[Ln(Iii)(2,6\text{-Dipicolinolate})_3]$ (Ln = Eu, Tb, or Its Solid Solutions). *Dalton Transactions* **2010,** *39*, 6483-6487.

50. Hardy, D. A.; Tigaa, R. A.; McBride, J. R.; Ortega, R. E.; Strouse, G. F. Structure–Function Correlation: Engineering High Quantum Yields in Down-Shifting Nanophosphors. *Journal of the American Chemical Society* **2019,** *141*, 20416-20423.
51. Irfanullah, M.; Sharma, D. K.; Chulliyil, R.; Chowdhury, A. Europium-Doped Laf_3 Nanocrystals with Organic 9-Oxidophenalenone Capping Ligands That Display Visible Light Excitable Steady-State Blue and Time-Delayed Red Emission. *Dalton Trans.* **2015,** ***44***, 3082-3091.
52. Binnemans, K. Interpretation of Europium(Iii) Spectra. *Coordination Chemistry Reviews* **2015,** *295*, 1-45.